Supporting Information

Discovery of novel 5-lipoxygenase activating protein (FLAP) inhibitors by exploiting a multistep virtual screening protocol

Abdurrahman Olgaç[a,b], Andrea Carotti[c], Christian Kretzer[d], Stephanie Zergiebel[d], Andreas Seeling[d], Ulrike Garscha[d], Oliver Werz[d], Antonio Macchiarulo[c*], Erden Banoglu[a,*]

[a] *Department of Pharmaceutical Chemistry, Faculty of Pharmacy, Gazi University, Etiler, 06560 Yenimahalle, Ankara, Turkey*

[b] *Laboratory of Molecular Modeling, Evias Pharmaceutical R&D Ltd., Gazi Teknopark G1-101, 06830, Golbasi, Ankara, Turkey*

[c] *Department of Pharmaceutical Sciences, University of Perugia, Via del Liceo 1, I-06123 Perugia, Italy*

[d] *Department of Pharmaceutical/Medicinal Chemistry, Institute of Pharmacy, Friedrich Schiller University Jena, Philosophenweg 14, 07743 Jena, Germany*

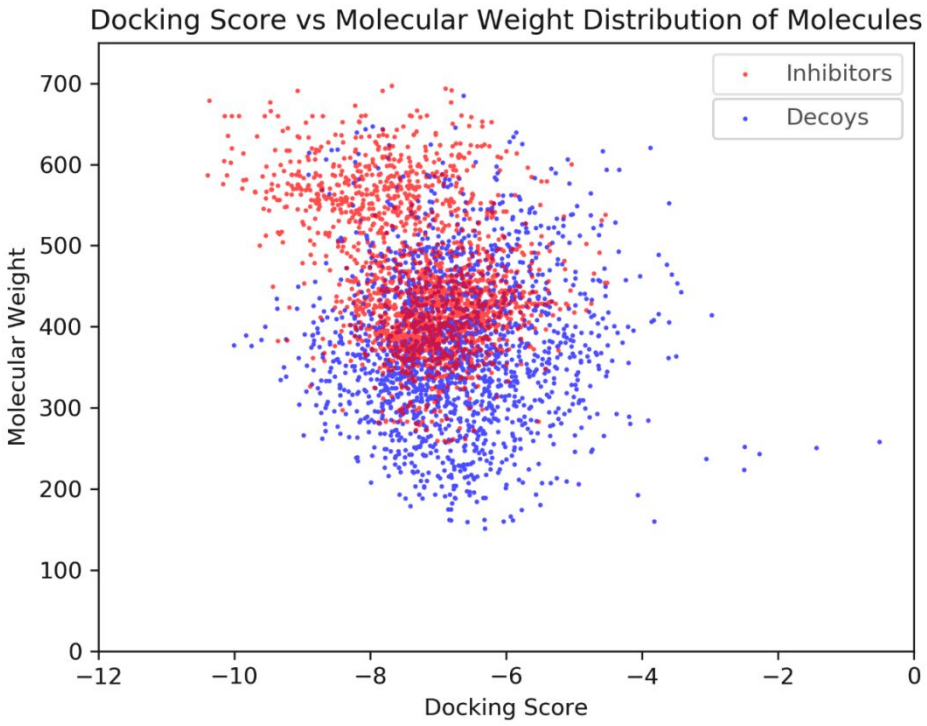

Figure S1. Comparison of the docking scores of 1968 potent FLAP inhibitors curated from ChEMBL database [1, 2] and 1918 molecules within Schrodinger Decoys Set [3], which was plotted against molecular weight as a basic paramater related with the molecular size.

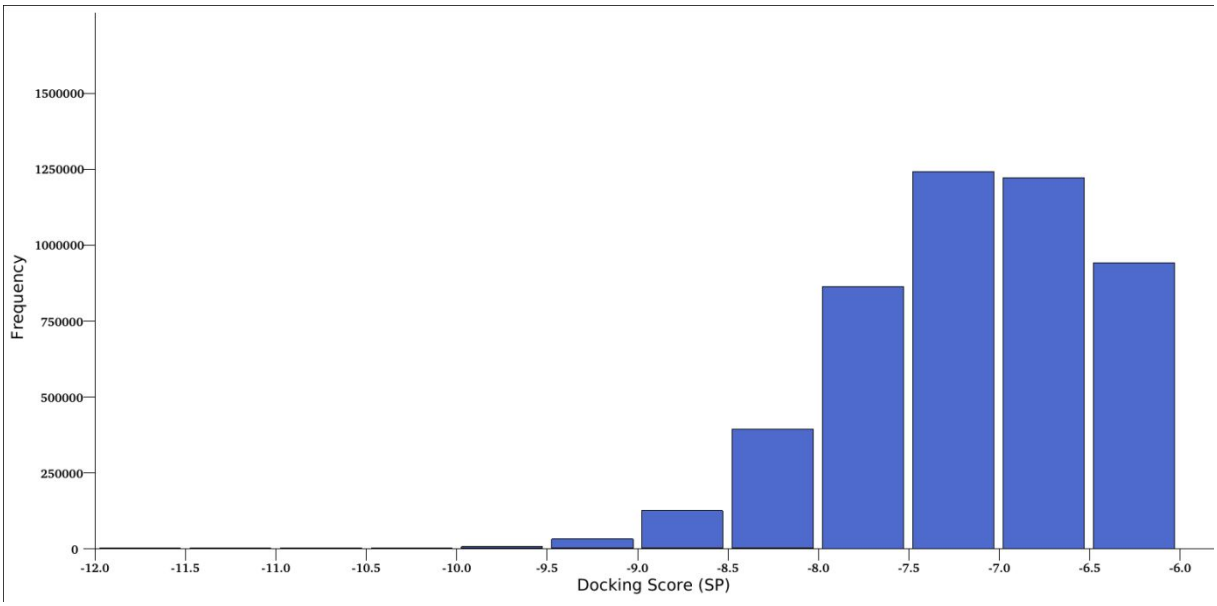

Figure S2. Docking score distribution after filtering the molecules from 6,255,980 unique molecules to 4,640,523 by docking scores lower than -6.

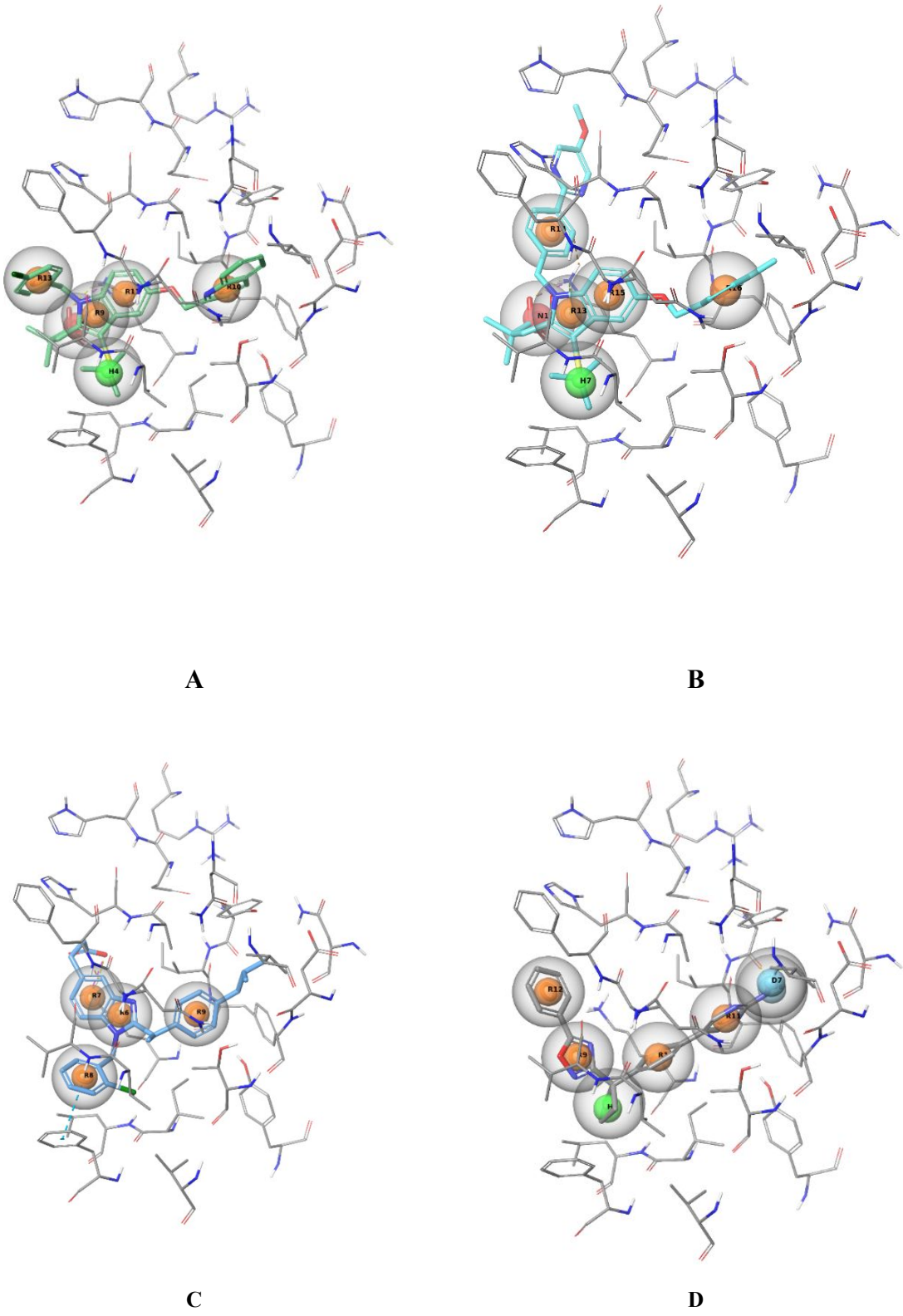

Figure S3. Visualization of the generated pharmacophore maps within FLAP active site by using Maestro [4].

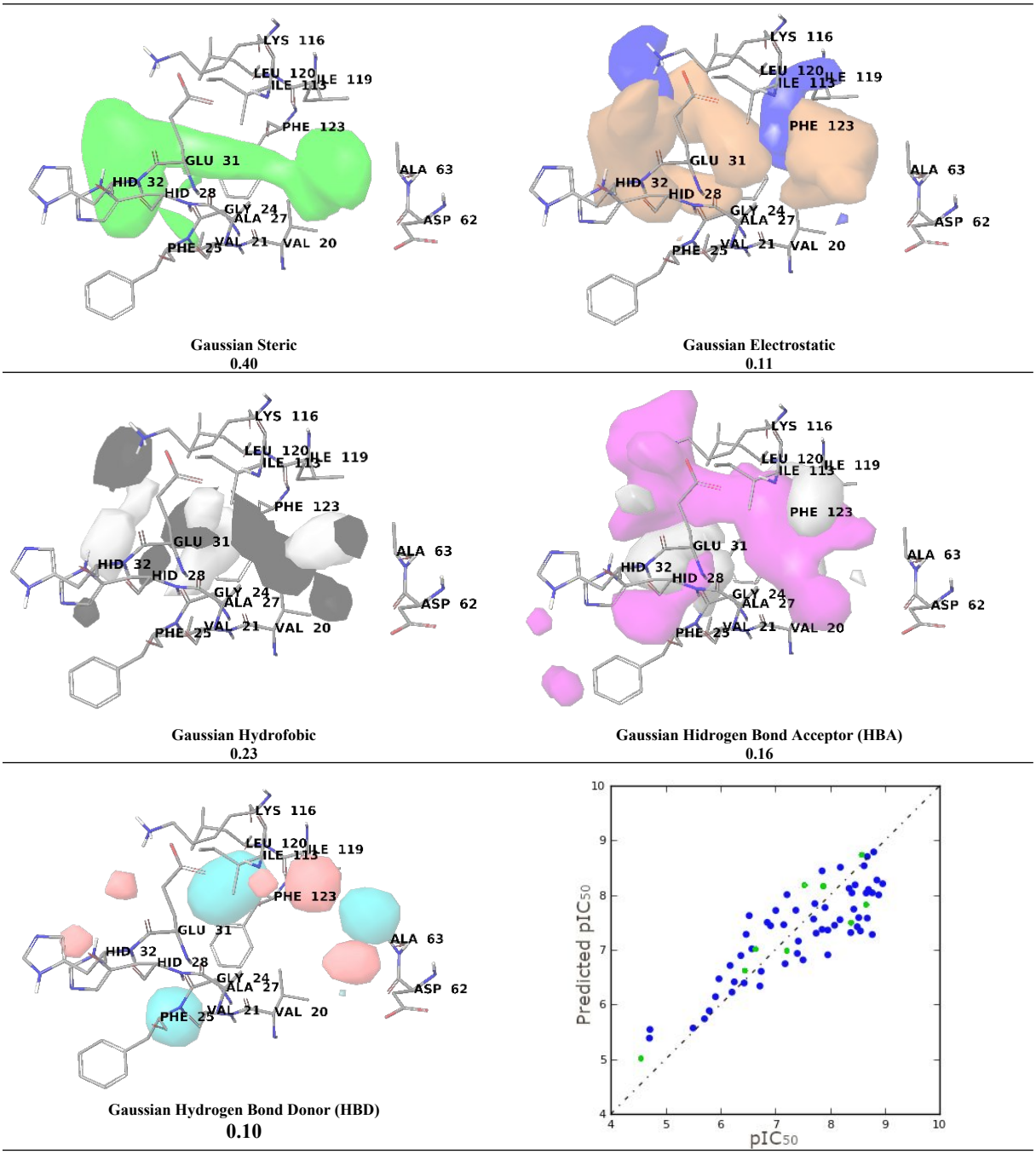

Figure S4. Representation of the 3D fields of each feature of the generated CoMSIA model given with their contributions of each feature on the 3D-QSAR model. A. Gaussian Steric, B. Gaussian Electrostatic, C. Gaussian Hydrophobic, D. Gaussian Hydrogen Bond Acceptor (HBA), E. Gaussian Hydrogen Bond Donor (HBD) F. Statistical results of the experimental and predicted pIC_{50} values of the molecules in training (blue) and test (green) sets.

Table S1. PLS Regression model validity and quality of the generated 3D-QSAR model.

r^2 (cross validation)	stability	F	P (chi square)	RMSE	q^2	pearson-r
0.84	0.91	326.5	$1.4e^{-28}$	0.21	0.71	0.88

Table S2. Statistical report of the classification model applied by Random Forest approach.

Real Classes		Predicted Classification		Correct Predictions		Incorrect Predictions	
Active	Inactive	Active	Inactive	Active	Inactive	Active	Inactive
247	20	228	39	227	19	1	20

Accuracy = % 92.13 % Error = % 7.87 Sensitivity = % 91.90 Selectivity = % 95.00

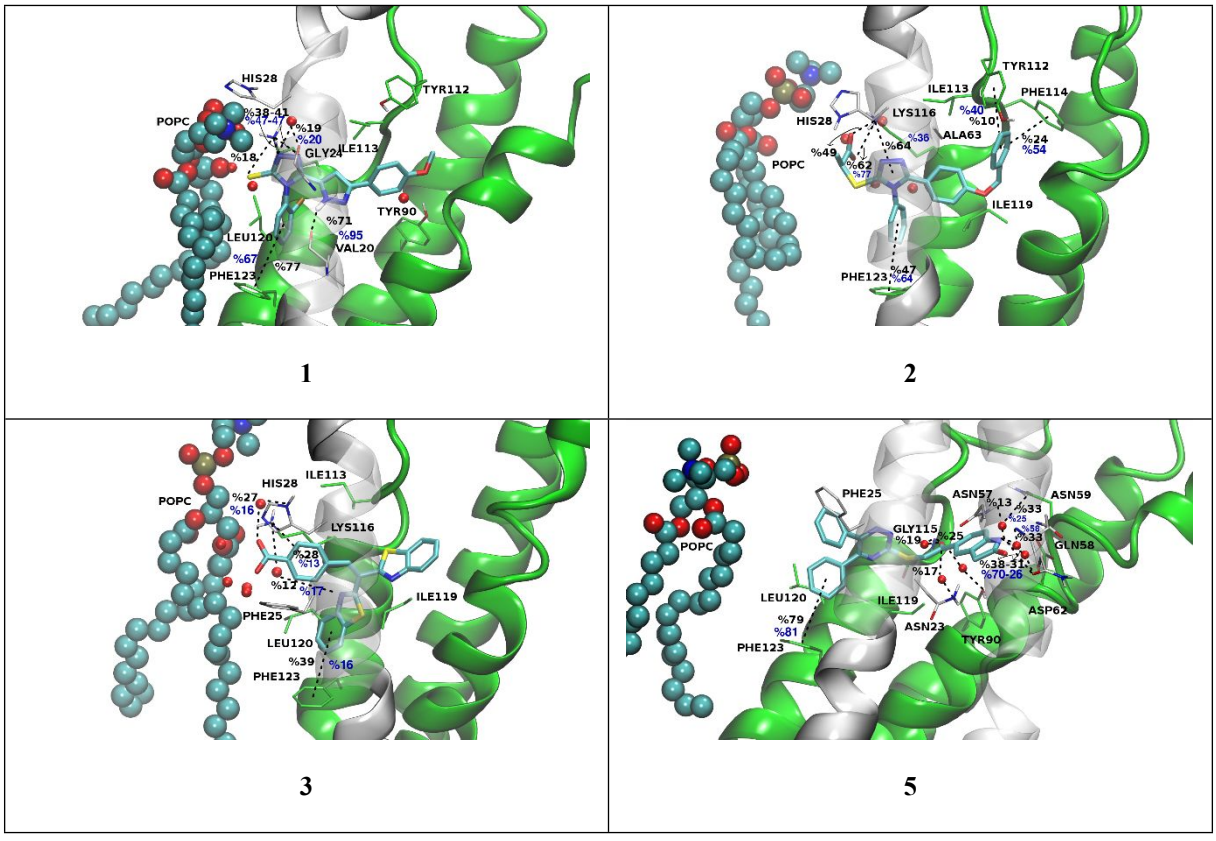

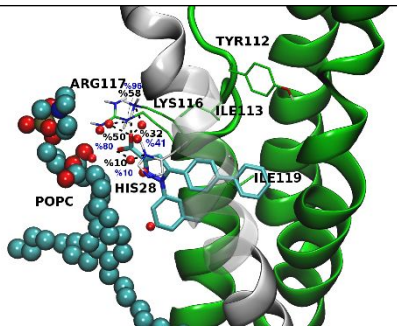	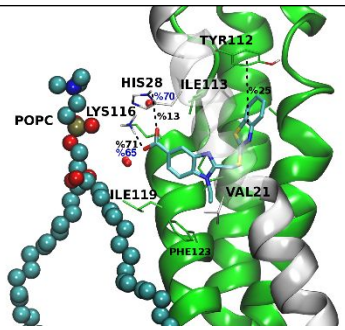
6	**7**
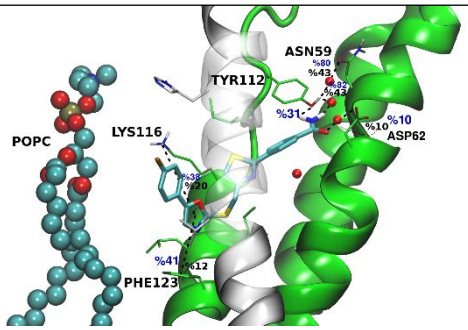	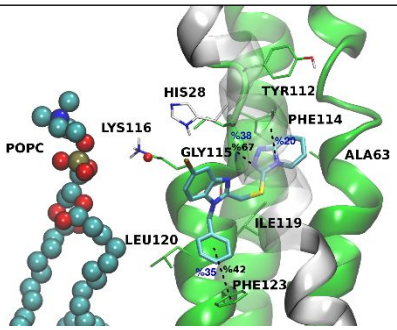
8	**9**
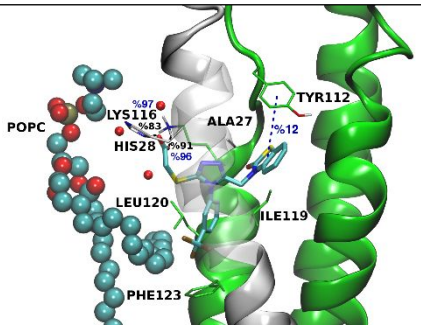	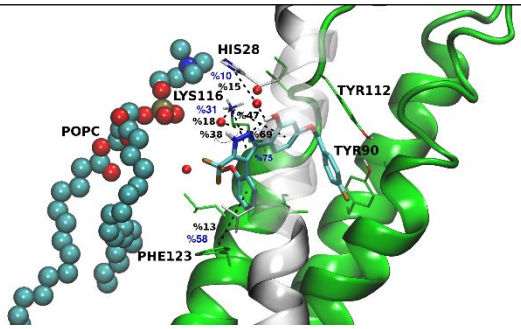
10	**12**
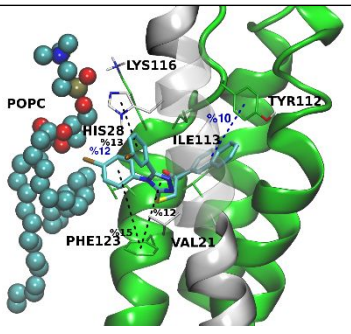	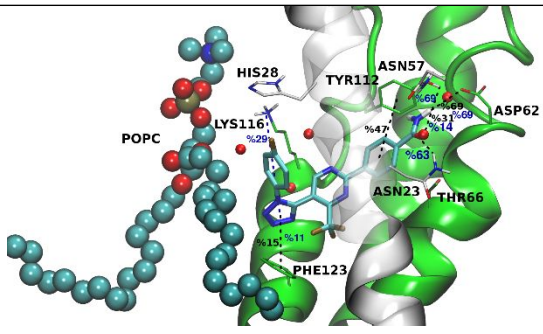
13	**14**

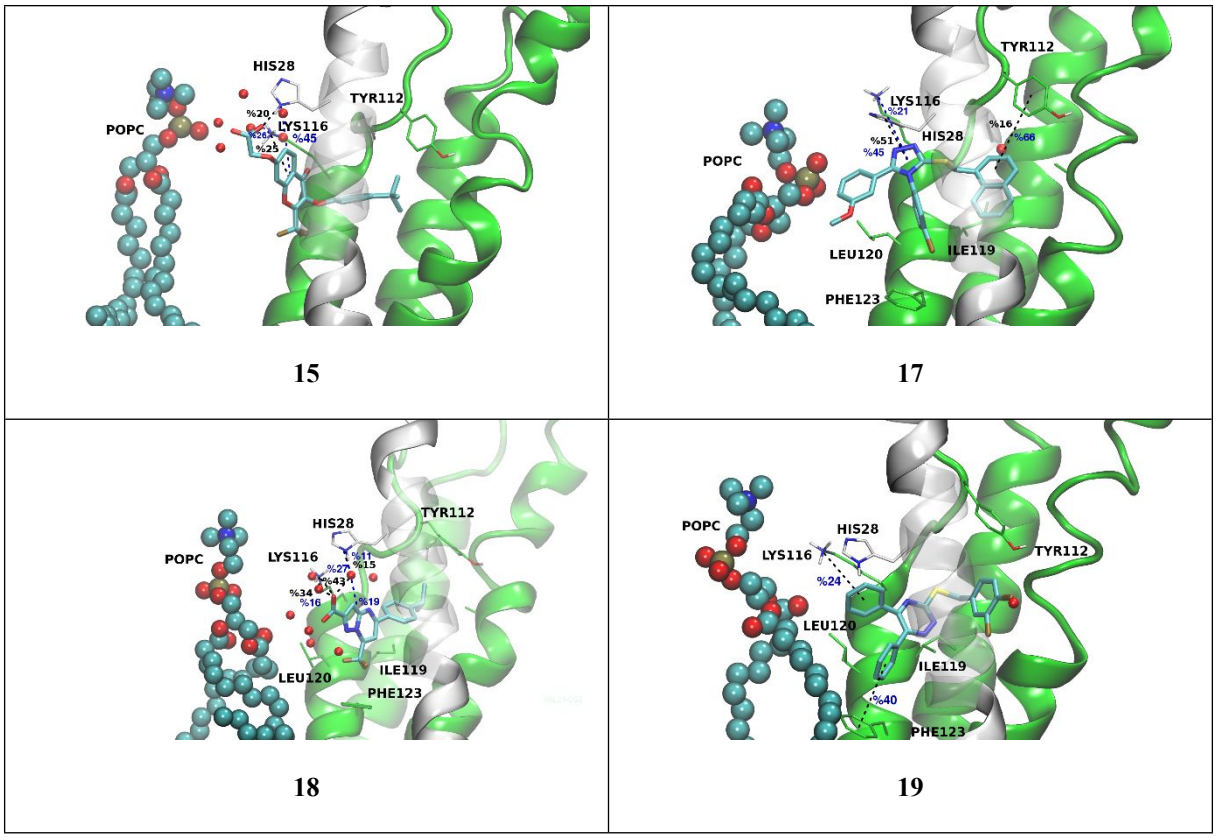

Figure S5. Schematic represantation of the main interactions of the selected compounds except 4, 11, 16, 20 (which are given at the main text) with FLAP considering membrane residues, the occupancies were calculated in the time window 0-10 ns (black) and 0-100ns (blue). The images were generated from a representative conformation of the most populated cluster of each simulation system.

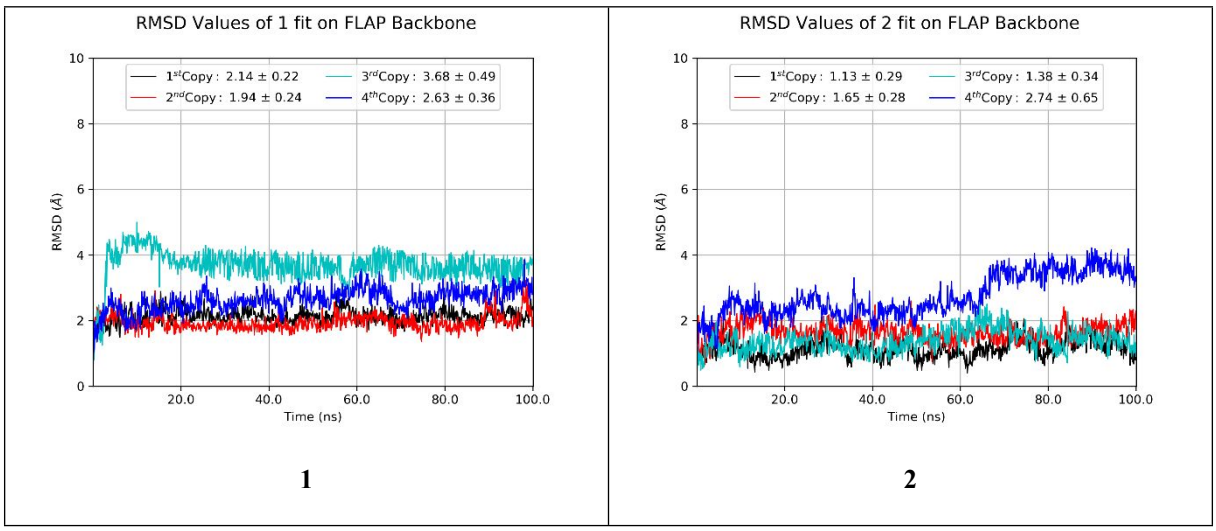

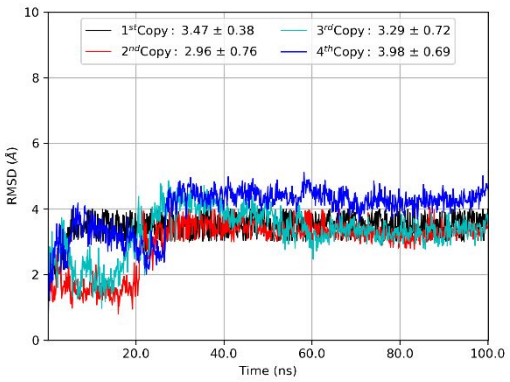
RMSD Values of 3 fit on FLAP Backbone
1st Copy : 3.47 ± 0.38
2nd Copy : 2.96 ± 0.76
3rd Copy : 3.29 ± 0.72
4th Copy : 3.98 ± 0.69
RMSD (Å)
Time (ns)

3

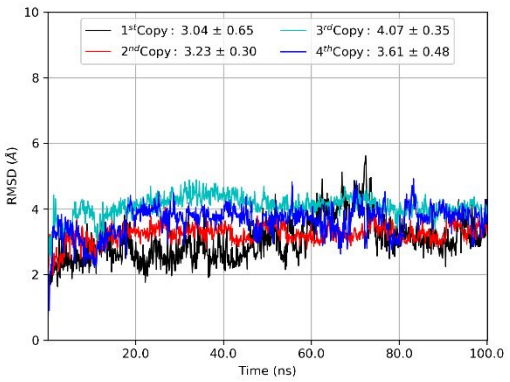
RMSD Values of 4 fit on FLAP Backbone
1st Copy : 3.04 ± 0.65
2nd Copy : 3.23 ± 0.30
3rd Copy : 4.07 ± 0.35
4th Copy : 3.61 ± 0.48
RMSD (Å)
Time (ns)

4

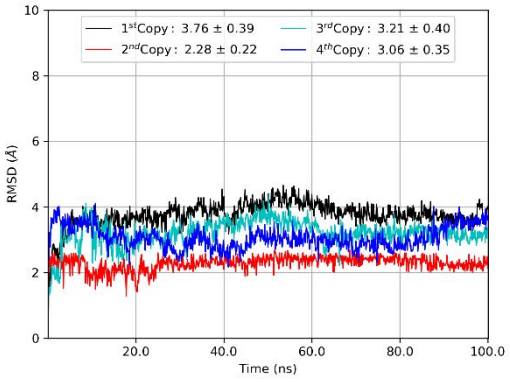
RMSD Values of 5 fit on FLAP Backbone
1st Copy : 3.76 ± 0.39
2nd Copy : 2.28 ± 0.22
3rd Copy : 3.21 ± 0.40
4th Copy : 3.06 ± 0.35
RMSD (Å)
Time (ns)

5

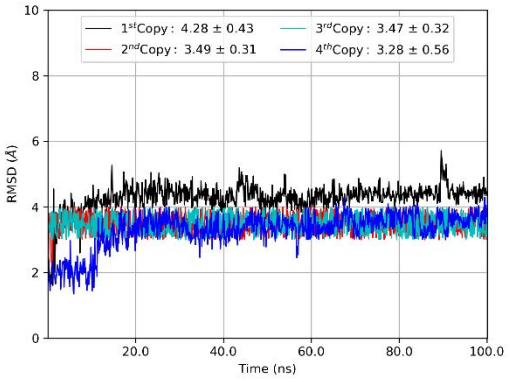
RMSD Values of 6 fit on FLAP Backbone
1st Copy : 4.28 ± 0.43
2nd Copy : 3.49 ± 0.31
3rd Copy : 3.47 ± 0.32
4th Copy : 3.28 ± 0.56
RMSD (Å)
Time (ns)

6

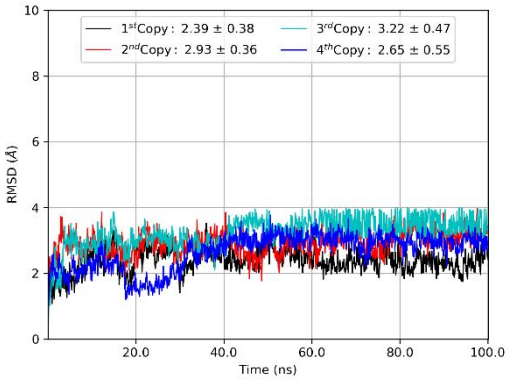
RMSD Values of 7 fit on FLAP Backbone
1st Copy : 2.39 ± 0.38
2nd Copy : 2.93 ± 0.36
3rd Copy : 3.22 ± 0.47
4th Copy : 2.65 ± 0.55
RMSD (Å)
Time (ns)

7

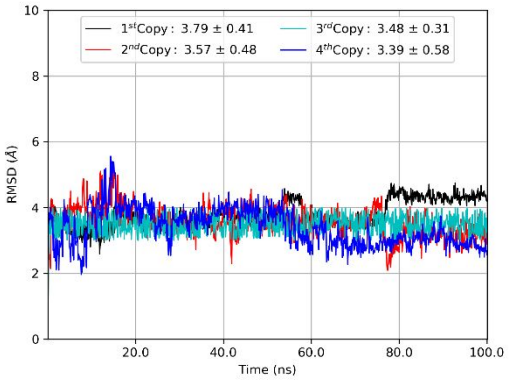
RMSD Values of 8 fit on FLAP Backbone
1st Copy : 3.79 ± 0.41
2nd Copy : 3.57 ± 0.48
3rd Copy : 3.48 ± 0.31
4th Copy : 3.39 ± 0.58
RMSD (Å)
Time (ns)

8

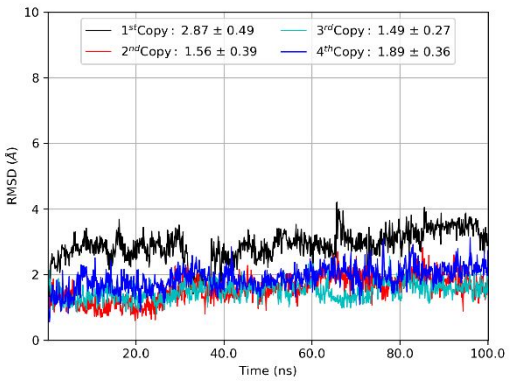

9

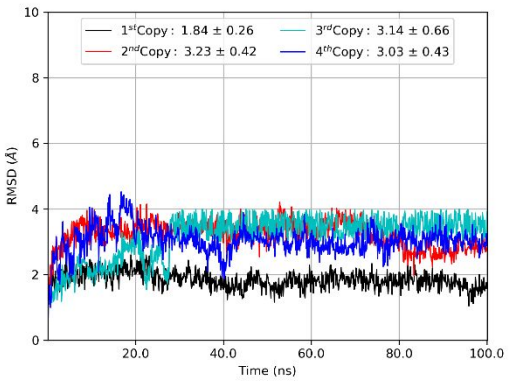

10

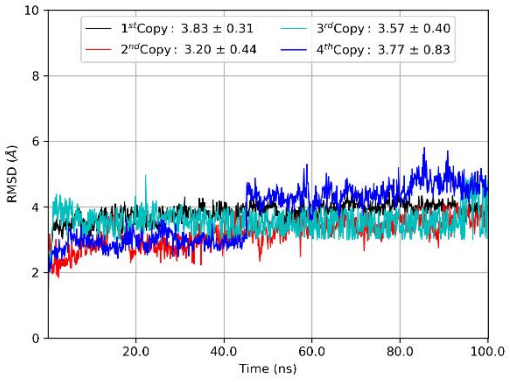

11

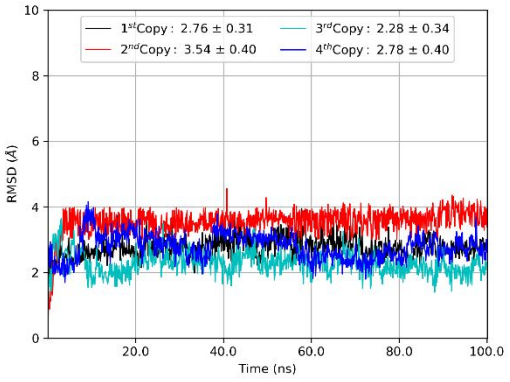

12

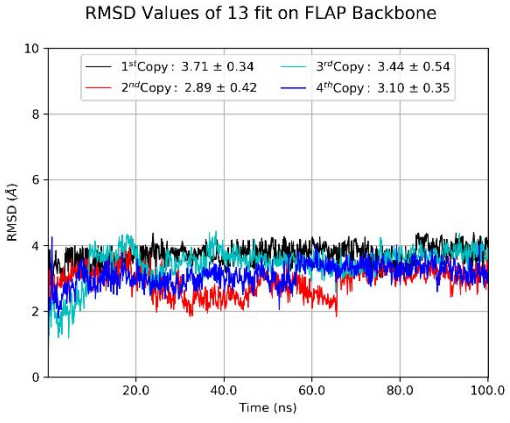

13

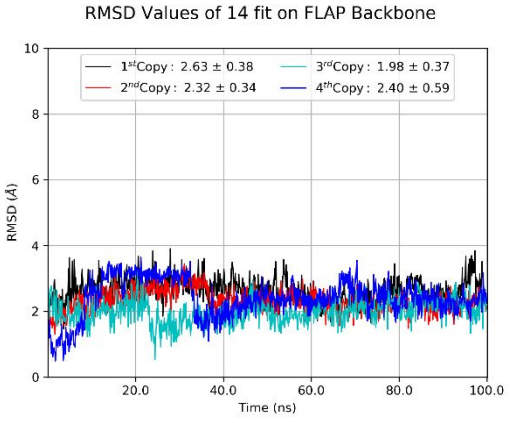

14

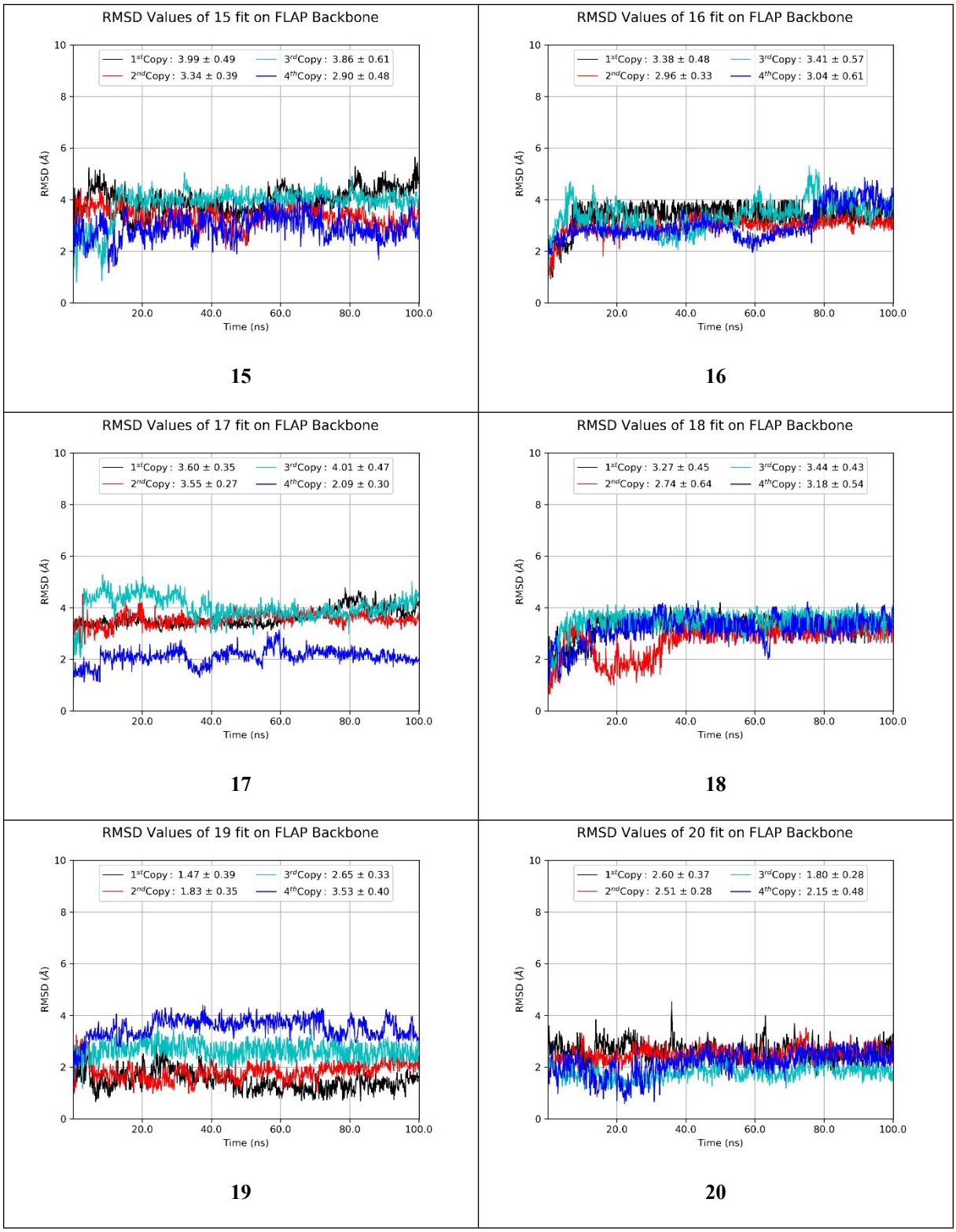

Figure S6. RMSD analyses of MD simulation were generated in complex with the virtual hit compound during, calculated by fitting on FLAP backbone.

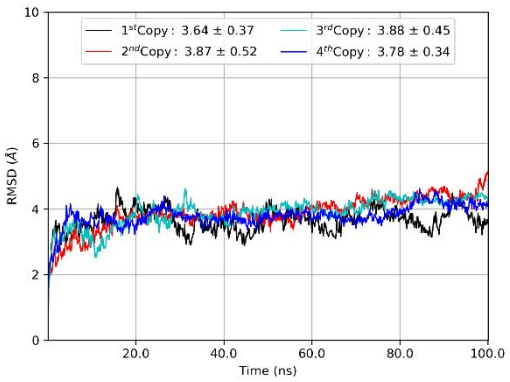
RMSD Values of FLAP Backbone, simulated with 1
1st Copy : 3.64 ± 0.37
2nd Copy : 3.87 ± 0.52
3rd Copy : 3.88 ± 0.45
4th Copy : 3.78 ± 0.34
RMSD (Å)
Time (ns)

1

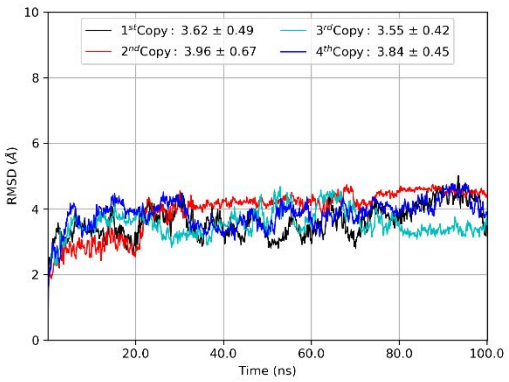
RMSD Values of FLAP Backbone, simulated with 2
1st Copy : 3.62 ± 0.49
2nd Copy : 3.96 ± 0.67
3rd Copy : 3.55 ± 0.42
4th Copy : 3.84 ± 0.45
RMSD (Å)
Time (ns)

2

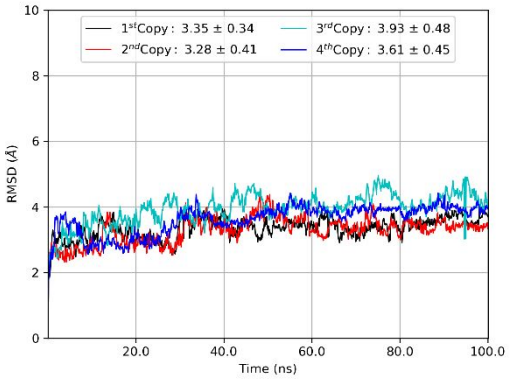
RMSD Values of FLAP Backbone, simulated with 3
1st Copy : 3.35 ± 0.34
2nd Copy : 3.28 ± 0.41
3rd Copy : 3.93 ± 0.48
4th Copy : 3.61 ± 0.45
RMSD (Å)
Time (ns)

3

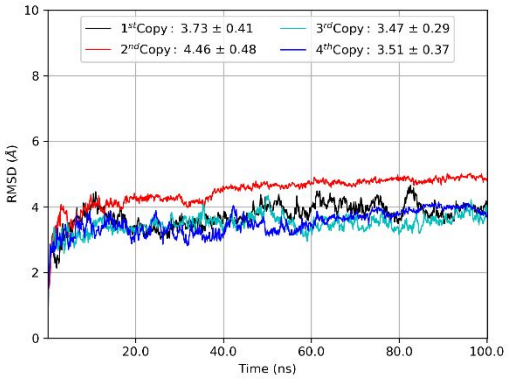
RMSD Values of FLAP Backbone, simulated with 4
1st Copy : 3.73 ± 0.41
2nd Copy : 4.46 ± 0.48
3rd Copy : 3.47 ± 0.29
4th Copy : 3.51 ± 0.37
RMSD (Å)
Time (ns)

4

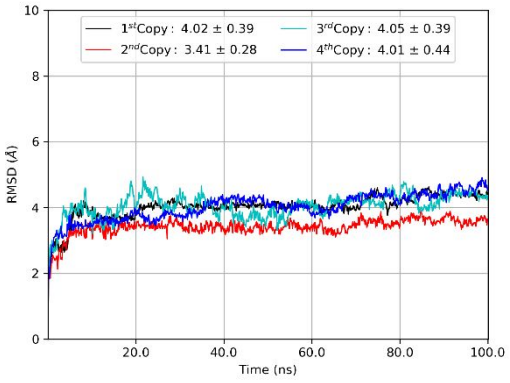
RMSD Values of FLAP Backbone, simulated with 5
1st Copy : 4.02 ± 0.39
2nd Copy : 3.41 ± 0.28
3rd Copy : 4.05 ± 0.39
4th Copy : 4.01 ± 0.44
RMSD (Å)
Time (ns)

5

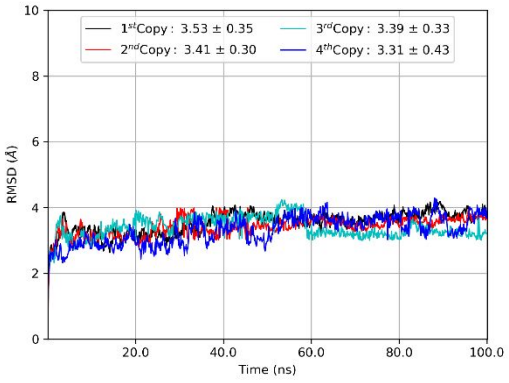
RMSD Values of FLAP Backbone, simulated with 6
1st Copy : 3.53 ± 0.35
2nd Copy : 3.41 ± 0.30
3rd Copy : 3.39 ± 0.33
4th Copy : 3.31 ± 0.43
RMSD (Å)
Time (ns)

6

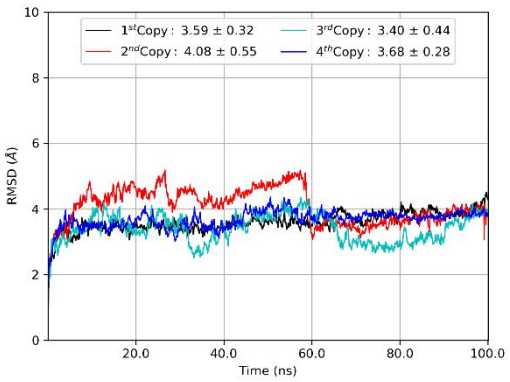
RMSD Values of FLAP Backbone, simulated with 7
1st Copy : 3.59 ± 0.32
2nd Copy : 4.08 ± 0.55
3rd Copy : 3.40 ± 0.44
4th Copy : 3.68 ± 0.28
RMSD (Å)
Time (ns)

7

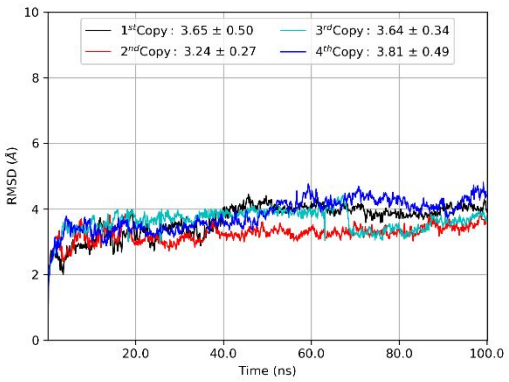
RMSD Values of FLAP Backbone, simulated with 8
1st Copy : 3.65 ± 0.50
2nd Copy : 3.24 ± 0.27
3rd Copy : 3.64 ± 0.34
4th Copy : 3.81 ± 0.49
RMSD (Å)
Time (ns)

8

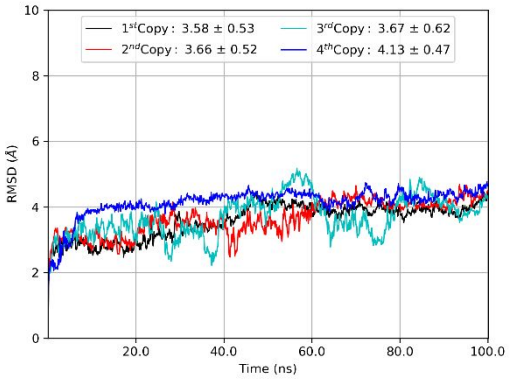
RMSD Values of FLAP Backbone, simulated with 9
1st Copy : 3.58 ± 0.53
2nd Copy : 3.66 ± 0.52
3rd Copy : 3.67 ± 0.62
4th Copy : 4.13 ± 0.47
RMSD (Å)
Time (ns)

9

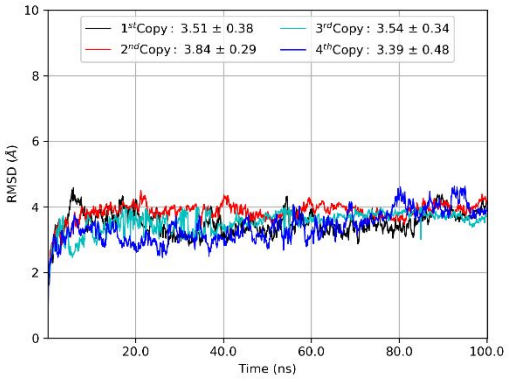
RMSD Values of FLAP Backbone, simulated with 10
1st Copy : 3.51 ± 0.38
2nd Copy : 3.84 ± 0.29
3rd Copy : 3.54 ± 0.34
4th Copy : 3.39 ± 0.48
RMSD (Å)
Time (ns)

10

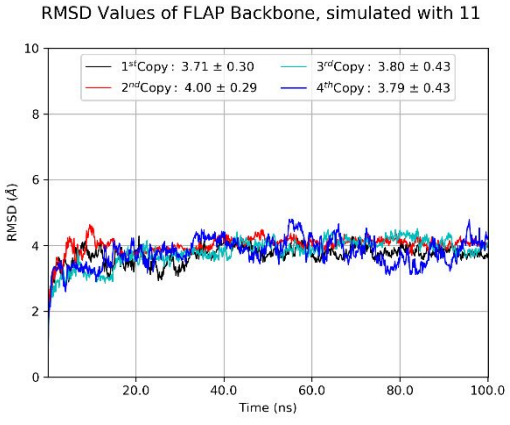
RMSD Values of FLAP Backbone, simulated with 11
1st Copy : 3.71 ± 0.30
2nd Copy : 4.00 ± 0.29
3rd Copy : 3.80 ± 0.43
4th Copy : 3.79 ± 0.43
RMSD (Å)
Time (ns)

11

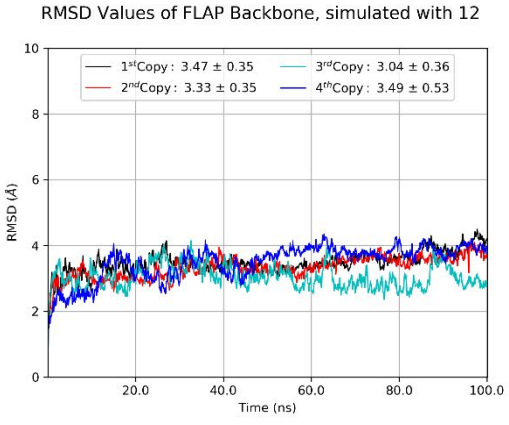
RMSD Values of FLAP Backbone, simulated with 12
1st Copy : 3.47 ± 0.35
2nd Copy : 3.33 ± 0.35
3rd Copy : 3.04 ± 0.36
4th Copy : 3.49 ± 0.53
RMSD (Å)
Time (ns)

12

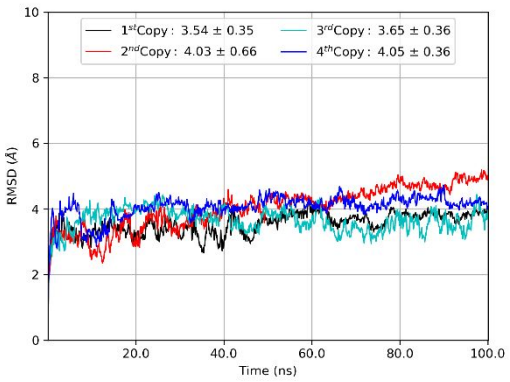

13

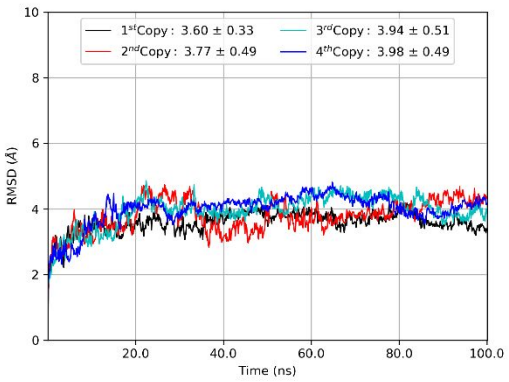

14

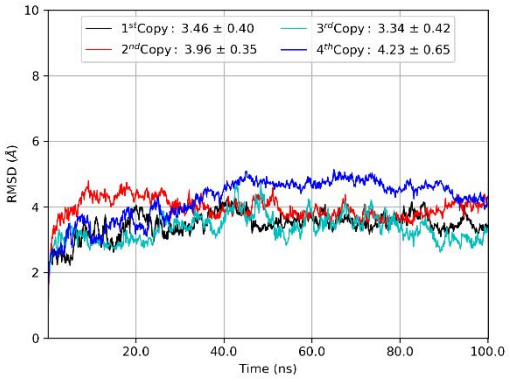

15

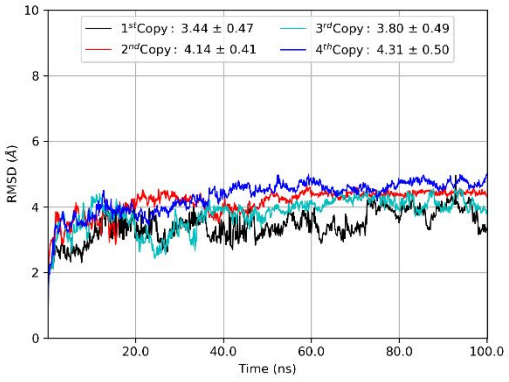

16

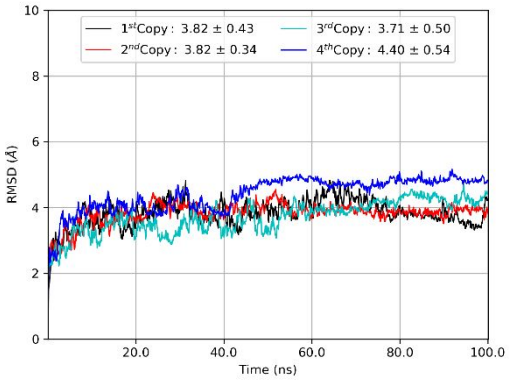

17

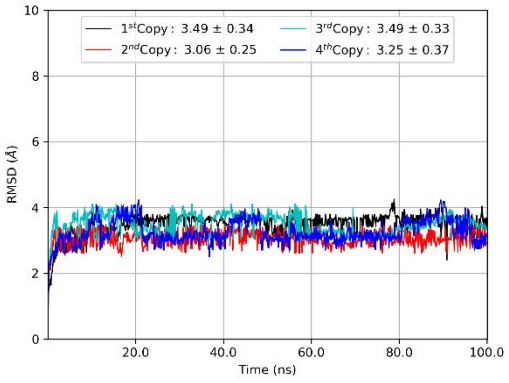

18

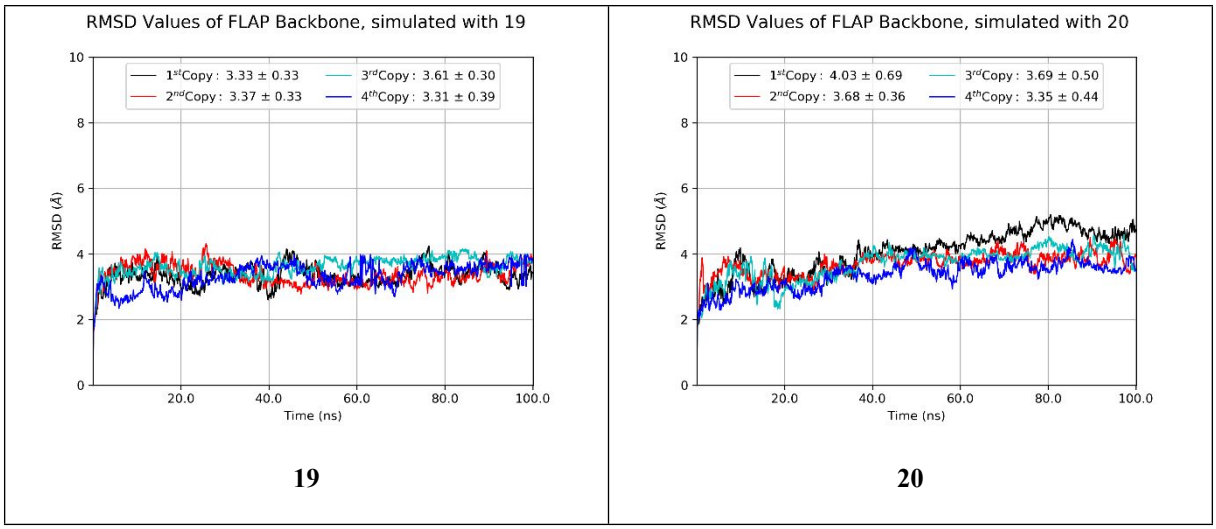

Figure S7. RMSD Analyses of FLAP backbone measured on each MD simulation system.

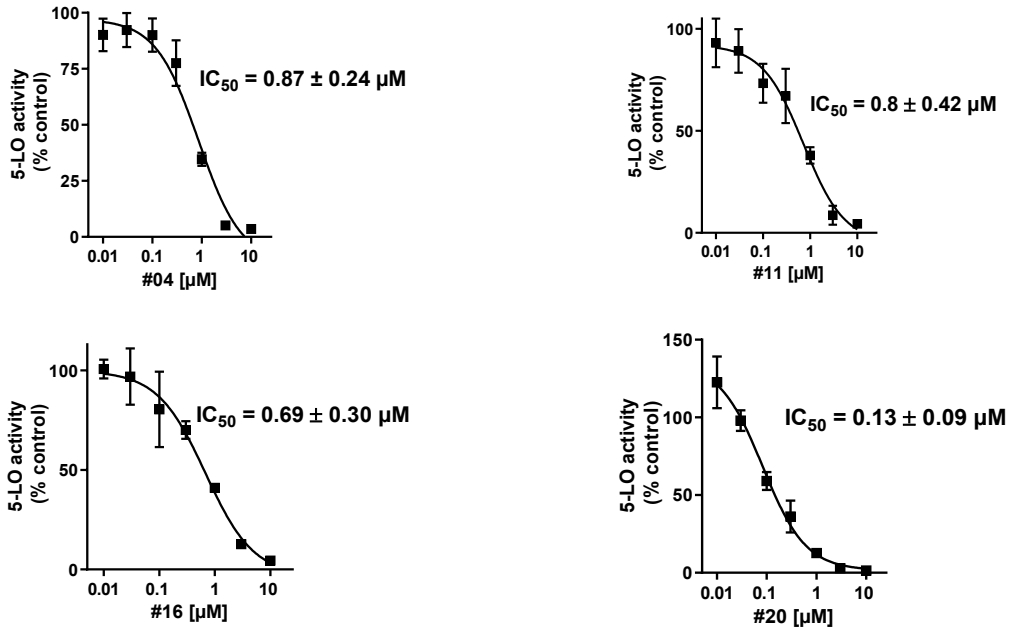

Figure S8. IC_{50} values retrieved by testing the compounds on polymorphonuclear leukocytes (PMNL) stimulated with 2.5 μM A23187.

	DMSO			#4			%	#11			%	#16			%	#20			%
5-HEPE	1063	±	290	150	±	124	14	27	±	13	3	57	±	22	5	246	±	123	23
5-HETE	24911	±	7143	3383	±	2447	14	960	±	509	4	1911	±	567	8	6048	±	2969	24
t-LTB_4	8151	±	2787	154	±	70	2	110	±	41	1	458	±	233	6	69	±	29	1
LTB_4	14847	±	5093	133	±	59	1	314	±	174	2	1084	±	388	7	32	±	15	0
5S,6R-diHETE	2585	±	1384	21	±	10	1	53	±	27	2	86	±	35	3	12	±	6	0
5,15 di-HETE	2585	±	1384	84	±	35	3	169	±	62	7	227	±	89	9	58	±	29	2
PGE_2	124	±	24	114	±	37	92	246	±	52	198	41	±	15	34	153	±	6	123
PGD_2	17	±	4	20	±	8	117	25	±	5	149	4	±	1	25	19	±	7	109
$PGF_{2\alpha}$	30	±	14	13	±	4	44	22	±	7	73	6	±	2	18	42	±	31	140
17-HDHA	39	±	8	30	±	6	76	27	±	5	68	21	±	2	53	28	±	9	71
15-HEPE	20	±	3	15	±	5	78	26	±	2	131	15	±	1	76	30	±	9	150
15-HETE	514	±	98	508	±	94	99	1013	±	245	197	492	±	54	96	1155	±	218	225
12-HETE	12072	±	2555	2868	±	859	24	9815	±	2803	81	8377	±	3141	69	12309	±	4688	102

Figure S9. Effects of test compounds on lipid mediator biosynthesis produced by 5-LO, COX, and 12/15-LO. PMNL were preincubated test compounds **4**, **11**, **16** and **20** (3 µM) for 10 min and stimulated with A23187 (2.5 µM) for another 10 min at 37 °C. Formed lipid mediators were analyzed by UPLC MS/MS. Values are given as mean in pg/5 x 10^6 PMNL ± SEM and as percentage in a heatmap (red colour indicates an increase, and blue colour a decrease), n=3.

Compound 4

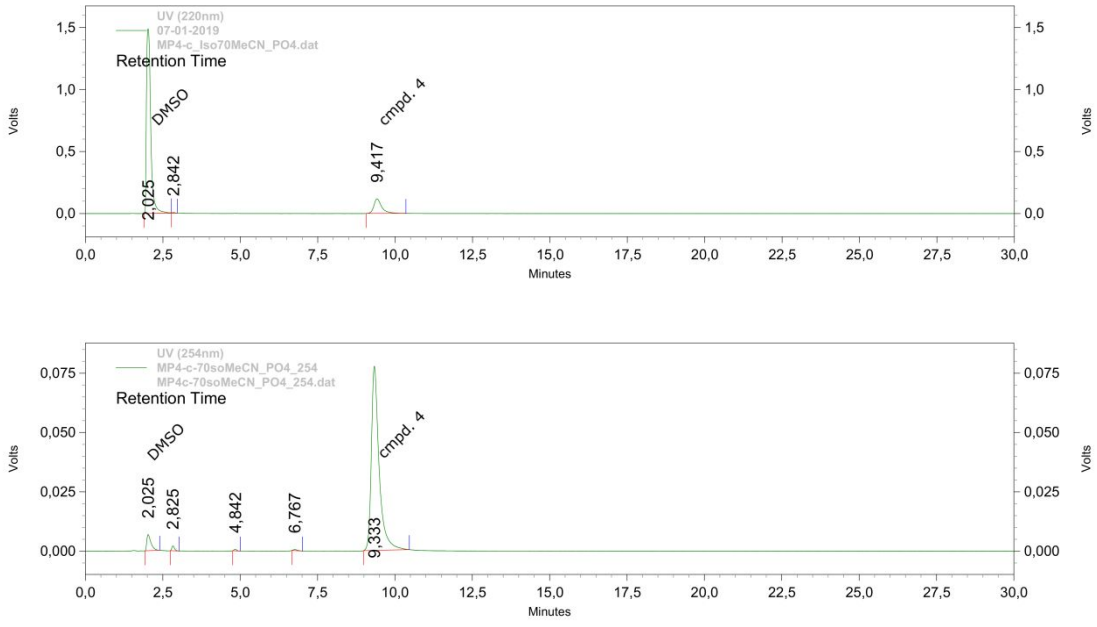

Compound 11

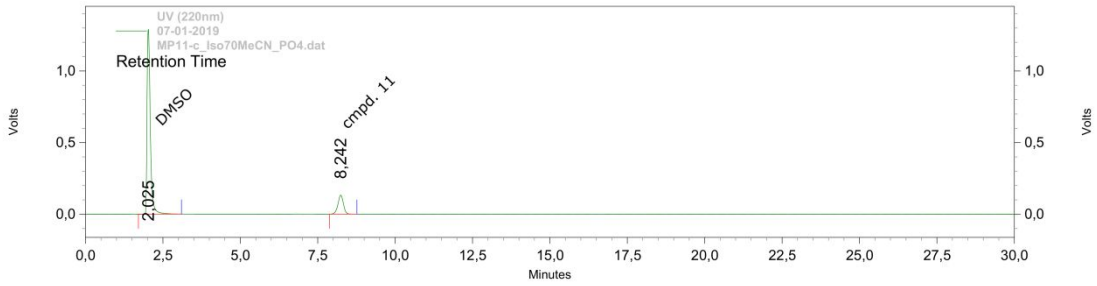

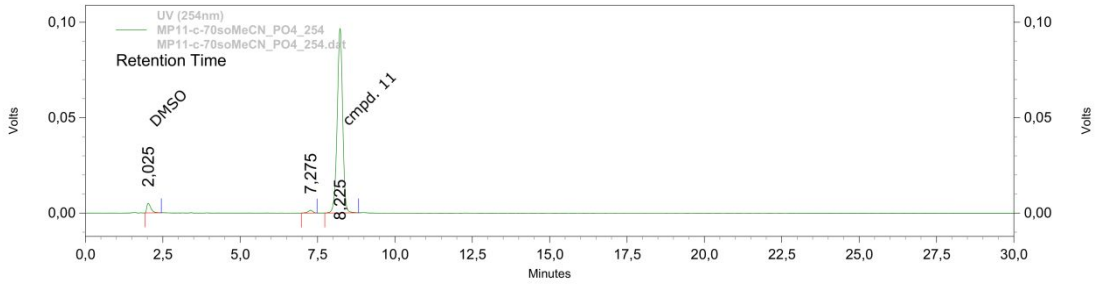

Compound 16

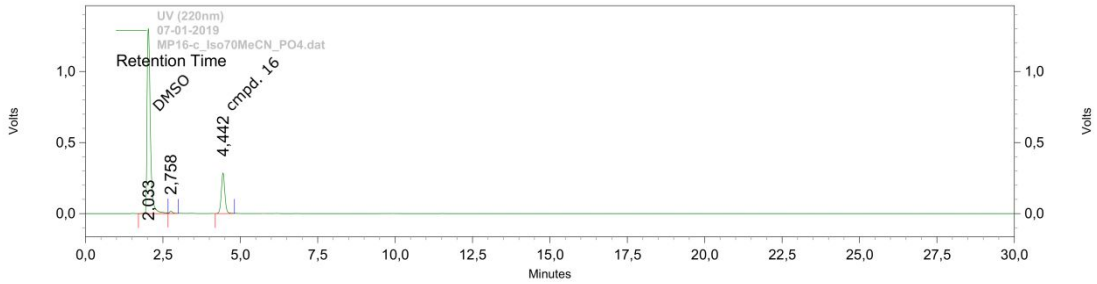

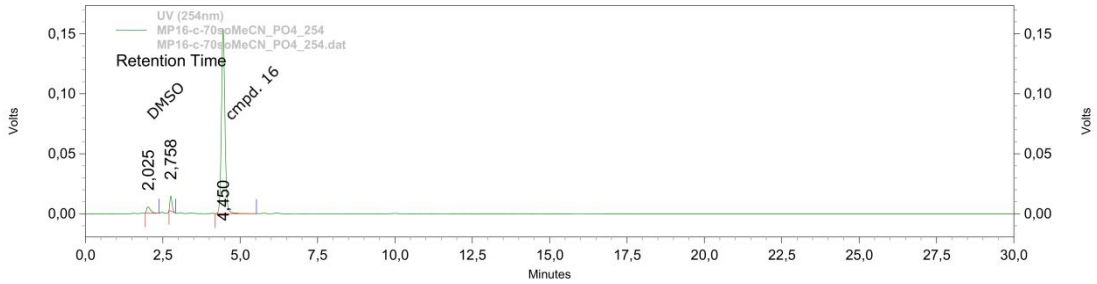

Compound 20

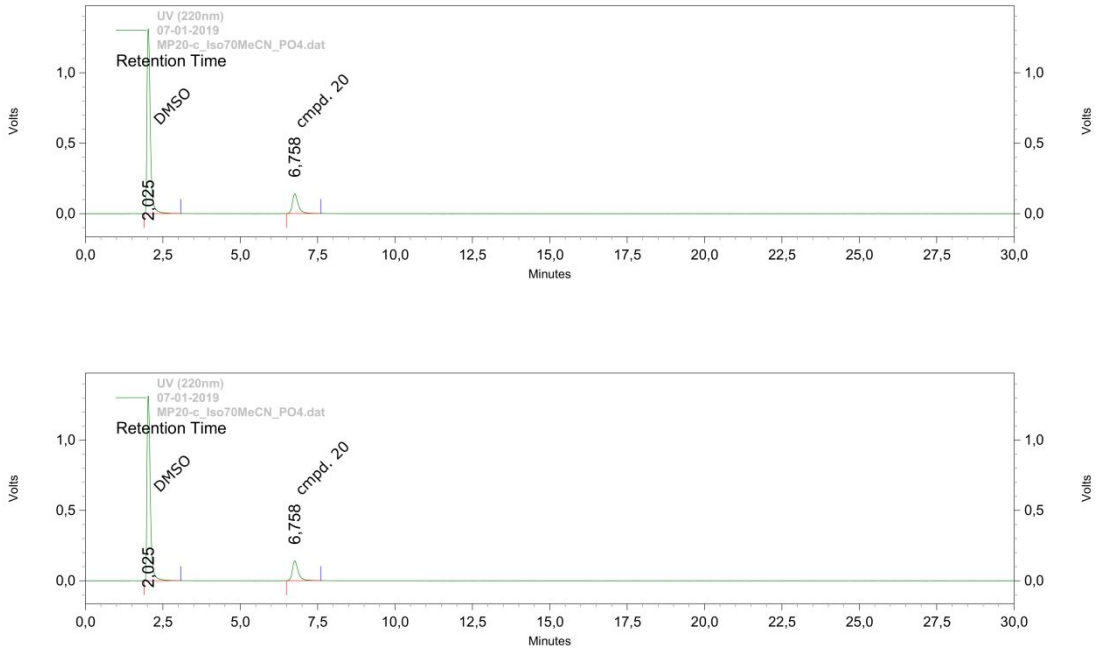

Figure S10. Purity analysis of compounds 4, 11, 16 and 20. Representative HPLC chromatograms for assessment of the purity of compounds 3, 11, 16, 20; chromatographic conditions: column, LiChroCART 250-4 (LiChrospher 100, RP18 ec, 5 µm, Merck); mobile phase, 70/30 (v/v%) ACN/50 mM KH_2PO_4 in H_2O (pH 3), flow rate, 1.0 mL·min^{-1}; column temperature, 20 °C; detection, UV at 220 nm and 254 nm, sample concentration: 0.1 mmol·L^{-1} compound.

Table S3. Cell-free 5-LO Inhibitory values of the compounds in intact neutrophils.

Compound	%5-LO Product Formation in Intact Neutrophils (Cell-free)		
	10 µM	1 µM	IC_{50} (µM)
4	40.89 ± 25.36	75.56 ± 12.93	>1
11	70.03 ± 7.20	74.32 ± 13.96	>10
16	44.34 ± 10.18	79.76 ± 9.11	>1
20	25.81 ± 6.66	31.09 ± 3.70	<1

Table S4. IUPAC Names, SMILES, Catalogue IDs of the hit compounds given with docking scores and matching pharmacophore model (PH4).

ID	IUPAC Name/SMILES	Catalogue IDs	Docking Score	PH4			
				1	2	3	4
1	4-(2-chlorophenyl)-5-(3-(4-methoxyphenyl)-1H-pyrazol-5-yl)-4H-1,2,4-triazole-3-thiol	ChemBridge Corp. 7551977	-7.066			X	
	COC1=CC=C(C=C1)C2=NNC(=C2)C3=NN=C(N3C4=CC=CC=C4Cl)S	MolPort-002-254-460					
2	2-((5-(4-(benzyloxy)phenyl)-4-phenyl-4H-1,2,4-triazol-3-yl)thio)propanoic acid	ChemBridge Corp. 7965019	-7.778			X	
	CC(C(=O)O)SC1=NN=C(C2=CC=C(C=C2)OCC3=CC=CC=C3)N1C4=CC=CC=C4	MolPort-002-292-304					
3	4-(2,2-bis(benzo[d]thiazol-2-yl)vinyl)benzoic acid	Enamine Ltd. Z46078163	-8.220			X	
	C1=CC=C2C(=C1)N=C(C(=CC3=CC=C(C=C3)C(=O)O)C4=NC5=CC=CC=C5S4)S2	MolPort-005-488-678					
4	3-benzyl-2-((3,4-dichlorobenzyl)thio)-4-oxo-3,4-dihydroquinazoline-7-carboxylic acid	Enamine Ltd. Z55881845	-7.279			X	
	C1=CC=C(C=C1)CN2C(=O)C3=C(C=C(C=C3)C(=O)O)N=C2SCC4=CC(=C(C=C4)Cl)Cl	MolPort-005-855-951					
5	5-(2-((5,6-diphenyl-1,2,4-triazin-3-yl)thio)acetyl)indolin-2-one	Enamine Ltd. Z65651568	-9.745				X
	C1=CC=C(C=C1)C2=NC(=NN=C2C3=CC=CC=C3)SCC(=O)C4=CC5=C(C=C4)NC(=O)C5	MolPort-005-769-658					
6	5-([1,1'-biphenyl]-4-yl)-1-(m-tolyl)-1H-pyrazole-3-carboxylic acid	Enamine Ltd. EN300-15058	-7.833	X	X	X	
	CC1=CC(=CC=C1)N2C(=CC(=N2)C(=O)O)C3=CC=C(C=C3)C4=CC=CC=C4	MolPort-002-470-086					
7	2-((benzo[d]thiazol-2-ylthio)methyl)-1-ethyl-1H-benzo[d]imidazole-5-carboxylic acid	Enamine Ltd. Z55180910	-7.742	X	X		
	CCN1C2=C(C=C(C=C2)C(=O)O)N=C1CSC3=NC4=CC=CC=C4S3	MolPort-004-007-343					
8	4-(4-(((5-(4-fluorophenyl)oxazol-2-yl)thio)methyl)thiazol-2-yl)benzamide	Enamine Ltd. Z803241874	-8.459				X
	C1=C(C=CC(=C1)C2=NC(=CS2)CSC3=NC=C(C4=CC=C(C=C4)F)O3)C(=O)N	MolPort-009-348-104					
9	3-(((1-benzyl-5-chloro-1H-benzo[d]imidazol-2-yl)methyl)thio)-[1,2,4]triazolo[4,3-a]pyridine	Enamine Ltd. Z295745992	-8.033			X	
	C1=CC=C(C=C1)CN2C3=C(C=C(C=C3)Cl)N=C2CSC4=NN=C5C=CC=CN54	MolPort-005-739-781					
10	2-((5-((2-oxobenzo[d]thiazol-3(2H)-yl)methyl)-4-(3-(trifluoromethyl)phenyl)-4H-1,2,4-triazol-3-yl)thio)acetic acid	Life Chemicals Inc. F0665-0820	-9.037		X		
	C1=CC=C2C(=C1)N(CC3=NN=C(N3C4=CC=CC=C4)C(F)(F)F)SCC(=O)O)C(=O)S2	MolPort-003-044-135					
11	2-((4-fluorobenzyl)thio)-5-(3-nitrophenyl)-1-(3-(trifluoromethyl)phenyl)-1H-imidazole	Life Chemicals Inc. F2964-3456	-7.499			X	X
	C1=CC(=CC(=C1)[N+](=O)[O-])C2=CN=C(N2C3=CC=CC(=C3)C(F)(F)F)SCC4=CC=C(C=C4)F	MolPort-009-698-915					
12	5-((4-fluorobenzyl)oxy)-2-(4-(2-methoxyphenyl)-3-(trifluoromethyl)-1H-pyrazol-5-yl)phenol	Pharmeks Ltd. PHAR150711	-7.298			X	
	COC1=CC=CC=C1C2=C(C3=C(C=C(C=C3)OCC4=CC=C(C=C4)F)O)NN=C2C(F)(F)F	MolPort-000-814-295					
13	2-((5-(3-chlorophenyl)-4-(4-chlorophenyl)-4H-1,2,4-triazol-3-yl)thio)-1-(naphthalen-2-yl)ethan-1-one	Pharmeks Ltd. PHAR362454	-8.384			X	
	C1=CC=C2C=C(C=CC2=C1)C(=O)CSC3=NN=C(C4=CC(=CC=C4)Cl)N3C5=CC=C(C=C5)Cl	MolPort-002-643-631					
14	4-(5-(1-(4-fluorophenyl)-1H-tetrazol-5-yl)-4-(trifluoromethyl)pyrimidin-2-yl)benzamide	Specs STK09617	-7.672	X		X	X
	C1=C(C=CC(=C1)C2=NC=C(C(=N2)C(F)(F)F)C3=NN=NN3C4=CC=C(C=C4)F)C(=O)N	MolPort-002-806-624					
15	2-((3-(4-(tert-butyl)phenoxy)-4-oxo-2-(trifluoromethyl)-4H-chromen-7-yl)oxy)acetic acid	Vitas-M Lab. STL330863	-7.943	X			
	CC(C)(C)C1=CC=C(C=C1)OC2=C(C(F)(F)F)OC3=C(C=CC(=C3)OCC(=O)O)C2=O	MolPort-000-652-148					
16	2-(((4-(4-methoxyphenyl)-5-(thiophen-2-yl)-4H-1,2,4-triazol-3-yl)thio)methyl)benzo[d]thiazole	Vitas-M Lab. STK807521	-7.637			X	
	COC1=CC=C(C=C1)N2C(=NN=C2SCC3=NC4=CC=CC=C4S3)C5=CC=CS5	MolPort-001-637-457					
17	4-(4-chlorophenyl)-3-(3-methoxyphenyl)-5-((naphthalen-1-ylmethyl)thio)-4H-1,2,4-triazole	Vitas-M Lab. STL054062	-8.155		X	X	

	COC1=CC=CC(=C1)C2=NN=C(N2C3=CC=C(C=C3)Cl)SCC4=CC=CC5=CC=CC=C54	MolPort-001-852-926					
18	5-(4-isopropylphenyl)-7-(trifluoromethyl)pyrazolo[1,5-a]pyrimidine-2-carboxylic acid	Vitas-M Lab. STL403648	-8.066	X	X		
	CC(C)C1=CC=C(C=C1)C2=NC3=CC(=NN3C(=C2)C(F)(F)F)C(=O)O	MolPort-001-645-799					
19	3-((3,4-dichlorobenzyl)thio)-5,6-diphenyl-1,2,4-triazine	Vitas-M Lab. STK096017	-7.494			X	
	C1=CC=C(C=C1)C2=NC(=NN=C2C3=CC=CC=C3)SCC4=CC(=C(C=C4)Cl)Cl	MolPort-000-496-908					
20	4,4'-((propane-2,2-diylbis(4,1-phenylene))bis(oxy))dianiline	Ark Pharm Inc. AK306875	-7.544				X
	CC(C)(C1=CC=C(C=C1)OC2=CC=C(C=C2)N)C3=CC=C(C=C3)OC4=CC=C(C=C4)N	MolPort-001-012-278					

References

1. Gaulton, A.; Hersey, A.; Nowotka, M.; Bento, A. P.; Chambers, J.; Mendez, D.; Mutowo, P.; Atkinson, F.; Bellis, L. J.; Cibrián-Uhalte, E.; Davies, M.; Dedman, N.; Karlsson, A.; Magariños, M. P.; Overington, J. P.; Papadatos, G.; Smit, I.; Leach, A. R., The ChEMBL database in 2017. *Nucleic Acids Res.* **2017**, 45, D945-D954.
2. Gaulton, A.; Bellis, L. J.; Bento, A. P.; Chambers, J.; Davies, M.; Hersey, A.; Light, Y.; McGlinchey, S.; Michalovich, D.; Al-Lazikani, B.; Overington, J. P., ChEMBL: a large-scale bioactivity database for drug discovery. *Nucleic Acids Res.* **2012**, 40, D1100-D1107.
3. Halgren, T. A.; Murphy, R. B.; Friesner, R. A.; Beard, H. S.; Frye, L. L.; Pollard, W. T.; Banks, J. L., Glide: a new approach for rapid, accurate docking and scoring. 2. Enrichment factors in database screening. *J. Med. Chem.* **2004**, 47, 1750-1759.
4. Schrödinger Release 2017-1: Maestro, S., LLC, New York, NY, 2017.
5. Gur, Z. T.; Caliskan, B.; Banoglu, E., Drug discovery approaches targeting 5-lipoxygenase-activating protein (FLAP) for inhibition of cellular leukotriene biosynthesis. *Eur. J. Med. Chem.* **2018**, 153, 34-48.